

# FRONTIERS IN MECHANICAL, MINING AND MATERIAL ENGINEERING

**ISSN: ( 3065- 4025 )**



[https://multisciajournals.com/  
journals/index.php/fmmme](https://multisciajournals.com/journals/index.php/fmmme)

[editor.fmmme@gmail.com](mailto:editor.fmmme@gmail.com)



## DEVELOPMENT OF FERRO-ALLOY HARDFACING FOR HIGH ABRASION AND LOW IMPACT WEAR APPLICATIONS

Chijioke Okechukwu<sup>1,3\*</sup>, Olurotimi Akintunde Dahunsi<sup>1</sup>,

<sup>1</sup>Department of Mechanical Engineering,

### Article Info

Received: 28-03-2025

Revised:03-04-2025

Accepted:14-04-2025

Published:26-04-2025

### Abstract

Extension of service lives of critical machine components subjected to wear is possible through application of hardfacing alloys. In this work, two hardfacing alloys were produced based on the mass ratios of 2: 1: 1 and 7: 1.5: 1.5 for Fe: Mn: Cr by sand and open permanent mold casting processes, respectively. XRD analysis of both samples showed the prominent presence of (Mn, Cr)<sub>23</sub>C<sub>6</sub>, (Fe, Mn, Cr)<sub>7</sub>C<sub>3</sub>, Cr<sub>3</sub>C<sub>2</sub>, Fe<sub>3</sub>C<sub>2</sub> and Fe<sub>4</sub>C carbides. Hägg carbide was prevalent in the SEM microstructural analysis of the sand cast sample, while cementite dominated the permanent mold cast sample. The average hardness values, impact energies absorbed and wear volumes of the samples produced with their respective charge mass ratios are 567 HV, 30 J and 0.131 cm<sup>3</sup> for 2: 1: 1 ratio and 592 HV, 29.5 J and 0.085 cm<sup>3</sup> for the 7: 1.5: 1.5 ratio. For service life applications as jaws, rolls, mantles, and concaves in crushers, the latter was recommended for manual metal arc welding to low carbon steel substrate because of its higher hardness, lower wear volume and cheaper alloy cost.

**Keywords:** hardfacing; service life; hardness; impact energy; wear volume.

### Introduction

Wear – a degradation phenomenon that adversely affects the useful life of components in machinery has become an inevitable challenge in many engineering applications. According to *Khanpara and Rathod* [1], wear is the predominant mechanism that controls the life of machine components as it makes components lose their dimensions and functionality. *Kenchi Reddy et al.* [2] noted that system variables, such as materials properties, environment, and mode of loading, influence the wear. *Haakonsen* [3] defined wear as the damage of solid surfaces due to removal or displacement of material by the mechanical action of a contacting solid, liquid or gas.

The optimum solution for extending the service life of components through improved wear resistance is applying surface wear resistant material to a cheaper and tougher core [4]. The method of improving the wear life of the component by overlaying a hard and wear resistant material on a substrate is known as “Hardfacing” [1]. Hardfacing alloys are usually made using carbide forming elements such as Ti, V, Cr, Mn, Fe, Zr, Nb, Mo, Hf, Ta, and W [5]. *Dolman* [6] and *Maroli et al.* [7] disclosed that higher carbide contents in the microstructure yield higher wear resistance.

Identification of underlying wear mechanism precedes reparation of worn surfaces. Conventional mechanisms of wear include abrasion, erosion, surface adhesion, surface fatigue, impact and corrosion [8, 9]. Selection or production of the hardfacing alloy is dependent on the identified mode of wear. Importantly, the nature of the substrate and the welding method that is suitable for joining the hardfacing alloy to the substrate need to be ascertained before hardfacing. Low alloy iron-based alloys containing up to a maximum of 12% alloy constituents and high alloy iron-based alloys containing 12 to 50% alloy constituents have been reported as categories of hardfacing alloys [10].

The use of commercially available hardfacing electrodes has been reported [11- 13]. Others mix powdered ferroalloys containing carbide forming elements with binders to form hardfacing compositions; for example, *Singh et al.* [14] recorded a maximum hardness value of 637 HV when 90%

Cr powder was mixed with sodium silicate and welded to mild steel by shielded metal arc welding.

The addition of free carbon powder to ferroalloy blend to increase the carbon content in the hardfacing weld is not useful since the free carbon does not readily dissolve in the molten weld pool during the short arc welding melting time to form hardfacing deposits on substrates. Mechanically mixing the metal powders does not yield homogeneous powder blend as segregation occurs during handling due to density differences between the ferroalloys. This density differences can lead to premature wear of the hardfacing in service due to non-uniform chemical composition and microstructure. The solution to these lies in the melting of the ferroalloy to obtain a homogeneous alloy composition [6].

Iron-based hardfacing alloys are used to resist abrasion and impact wear of critical components in mineral processing applications [7]. Examples of recently hardfaced components in this sector include tangential rotary picks [15], and cone pick cutters [16].

The objectives of this research are to develop economical hardfacing ferroalloys and select preferred substrate material for high abrasion and low impact wear applications, to evaluate the wear properties of the hardfacing alloys, and to select the preferred hardfacing composition based on the wear properties and cost.

### **Materials and methods**

Materials used for the production of ferroalloy hardfacing were ferromanganese (FeMn), ferrochrome (FeCr) and cast iron. FeMn was chosen because Mn increases the impact property of ferrous alloys [17], while FeCr was used because high amount of chromium in hardfacing increases carbide formation, which increases the hardness value [18]. Cast iron was used to supplement the iron and carbon content of the ferroalloys in the hardfacing. Low carbon steel was selected as a substrate due to its high impact energy [19] and excellent weldability. In this research, two hardfacing alloys were produced based on the mass charge ratio of 2: 1: 1 and 7: 1.5: 1.5 for Fe: Mn: Cr by sand and open permanent mold casting processes, respectively.

Methods used for researching the desired properties required for wear application of hardfacing samples are the following: scanning electron microscopy (SEM) with energy dispersive spectroscopy (EDS); X-ray diffraction analysis; hardness measurements; wear and impact tests.

Combined scanning electron microscopy (SEM) and energy dispersive spectroscopy (EDS) were carried out to examine the microstructure of the hardfacing samples. The cut samples were ground with abrasive papers of grits 220, 400, 800 and 1200. Polishing of the ground samples was done with aluminum oxide powder, which was spread on the polishing cloth and wetted, while the speed of rotating disc was from 350 to 400 rpm to achieve mirror surface. Etching of the polished surface was achieved with Nital reagent to reveal the microstructural details of the samples before the SEM.

Additionally, each sample was put on a holder and positioned in the SEM before the illumination of the etched surfaces at a magnification of 400; photomicrographs were generated at this magnifications. Also, EDS was carried out at a magnification of 400, and the spectra of the samples were generated. A combination of SEM and EDS was used to generate the composition, quantification percentage error, and certainty of selected elements.

The prepared samples were held in the universal sample holder and analyzed with a PAN analytical Empyrean diffractometer with PIXcel detector and fixed slits with Fe filtered Co-K $\alpha$  radiation. The phases were identified partly with X'Pert Highscore plus and partly with crystallographic search-match software.

A digital hardness testing machine (INDENTEC) was used to determine the hardness of the experimental samples 1 and 2. The surface of the sample was flattened with a bench grinder before indentation. Rockwell-C hardness values were read from the machine, while the average value was converted to Vickers hardness.

The wear behavior of the hardfacing compositions was investigated with Struers Rotopol-V wear tester. Mass of each hardfacing sample was measured before and after the wear period of 1800 s, in a Denver digital scale. Abrasive paper of grit-220 was used, and the speed of disc was 300 rpm. Given that  $m_L$  (g) is the mass loss,  $\rho$  is the density of the material ( $\text{g}/\text{cm}^3$ ), *Scandella and Bonnel* [4] reported that mass losses could be converted to volume losses using the equation:

$$\text{Wear volume} = \frac{m_L}{\rho} \quad 1$$

Charpy impact test of the samples was carried out on the hardfaced samples. The test samples were prepared by joining mild steel plate to the hardfacing samples by manual metal arc welding and grinding to 10 mm x 10 mm x 60 mm; each component of the mild steel and hardfacing sample had a dimension of 5 mm x 10 mm x 60 mm. A V-notch of depth 2.5 mm was made at the center of the surface of the mild steel substrate. The maximum velocity of the impact hammer was 5.24 m/s.

### Results and discussions

Preceding the selection of an economical hardfacing composition, the composition of the hardfacing samples 1 and 2, their carbide phases, hardness values, wear volumes, impact energies and microstructures were determined. Microstructural details of the sample were investigated with SEM, while carbides of Fe, Mn, and Cr were detected with X-ray diffractometer.

#### *Compositions and alloy contents of the hardfacing samples*

The concentrations of samples 1 and 2 and their corresponding percentage certainty are shown in Table 1. These results were generated using the combined SEM and EDS.

*Table 1 Chemical composition and certainty of hardfacing sample 1 and 2*

Element	Sample 1		Sample 2	
	Wt. (%)	Certainty (%)	Wt. (%)	Certainty (%)
Fe	52.5	98.7	69.1	98.8
Mn	28.9	98.4	14.0	97.5
Cr	9.8	97.4	11.1	97.6
Si	1.9	94.7	1.5	93.8
C	0.9	94.1	1.3	95.0
Ni	0.9	75.1	0.0	100.0
Mo	0.7	79.4	2.0	91.6
Ti	0.3	61.5	0.4	77.1
V	0.2	33.5	0.5	74.6
W	3.9	73.7	0.0	100.0

Sample 1 has 47.5 %, while sample 2 has 30.9 % of alloying elements. From the composition analysis, it can be seen that the wt.% of iron and manganese were closer to the mass ratio values than that of chromium. For example, for the 2: 1: 1 of Fe, Mn, and Cr the wt.% were 52.5, 28.9 and 9.8, respectively; and for the 70: 15: 15 of Fe, Mn, and Cr, the wt.% were 69.1, 14, and 11. This relation indicates that Fe and Mn melt faster to form the alloy, while the melting and alloying of chromium delay.

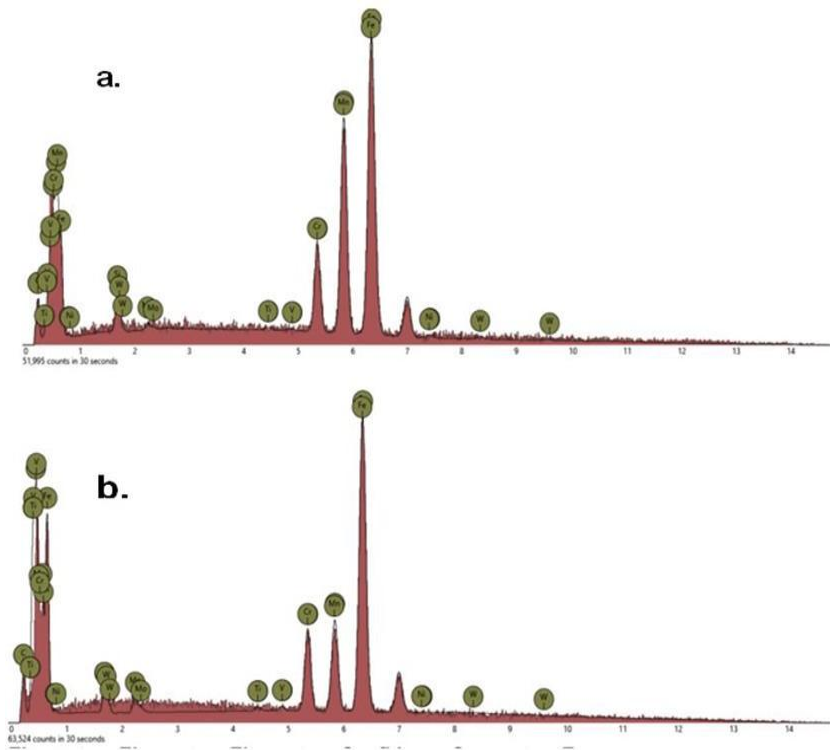


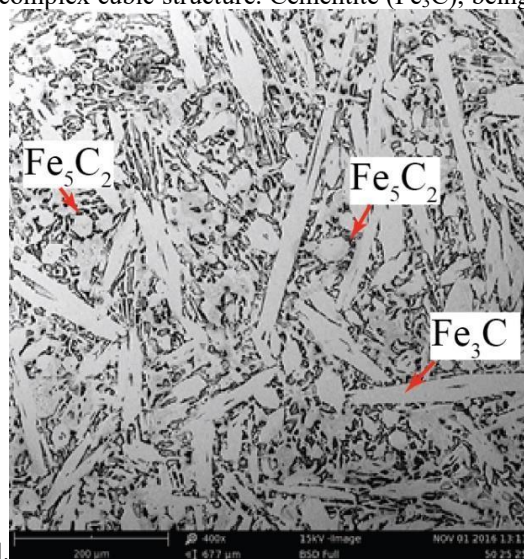
Fig. 1. EDS of a) sample 1, and b) EDS of sample 2.

The EDS results showed that iron was prevalent in both samples 1 and 2, followed by manganese and chromium (Fig. 1). Elements such as Mo, Ni, W, Ti and V with low certainty percentage were not considered as these were insignificant in the actual compositions of the charge materials.

*Microstructures of the hardfacing samples and their carbide phases*

Microstructures of samples 1 and 2 as revealed by SEM are shown in Fig. 2a and Fig. 2b, respectively. According to *Ande* [20], the crystal structure of Hägg carbide ( $\text{Fe}_5\text{C}_2$ ) is still under debate; however, the iron atoms in  $\chi\text{-Fe}_5\text{C}_2$  are in distorted sheets of hexagonal arrangements [21]. The high carbon steel or tool steels tempering between 200 °C and 300 °C results in the precipitation of Hägg carbide ( $\text{Fe}_5\text{C}_2$ ) [22, 23]. Hence, the prevalence of the metastable hexagonal prism-shaped Hägg carbide in sample 1 arose due to solidification and cooling in sand molds.

*Serna et al.* [24] noted that  $\text{M}_3\text{C}$  carbides have an orthorhombic crystal structure,  $\text{M}_7\text{C}_3$  are hexagonal, while  $\text{M}_{23}\text{C}_6$  carbides show complex cubic structure. Cementite ( $\text{Fe}_3\text{C}$ ), being orthorhombic



forms directly from the melt in cast iron [23].

Consequently, cementite –a more stable carbide than Hägg carbide dominated the microstructure of sample 2 and showed consistent presence in sample 1

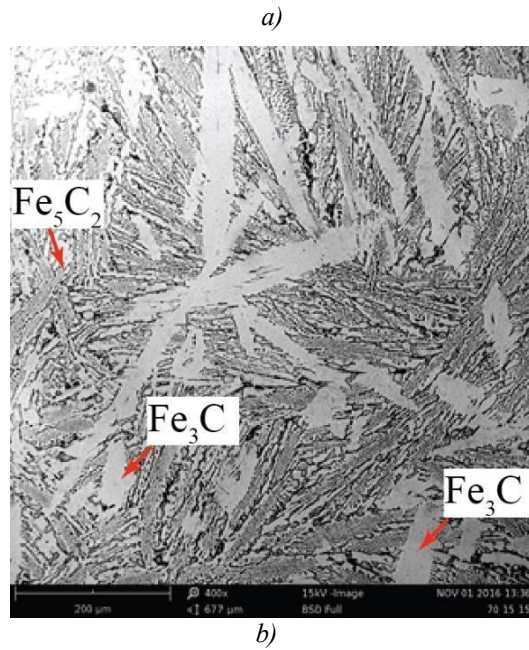
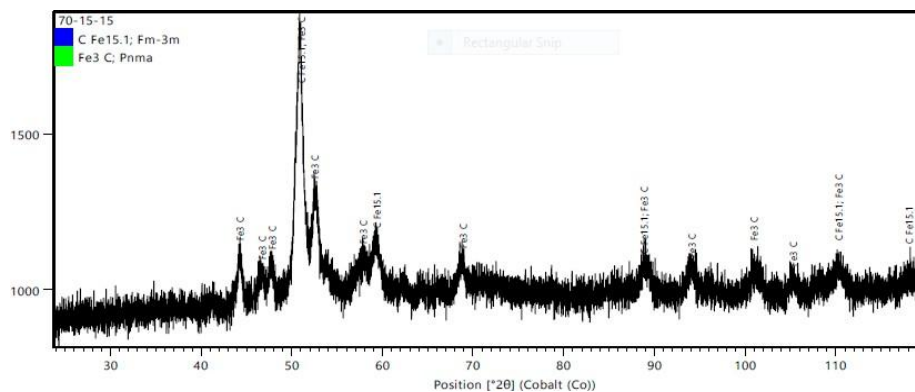
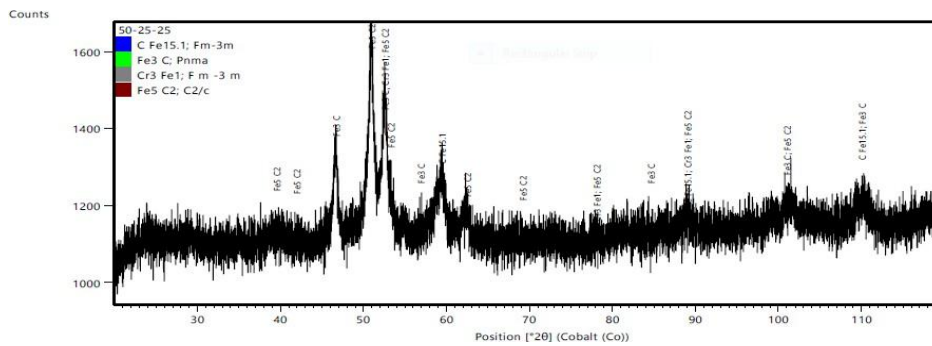


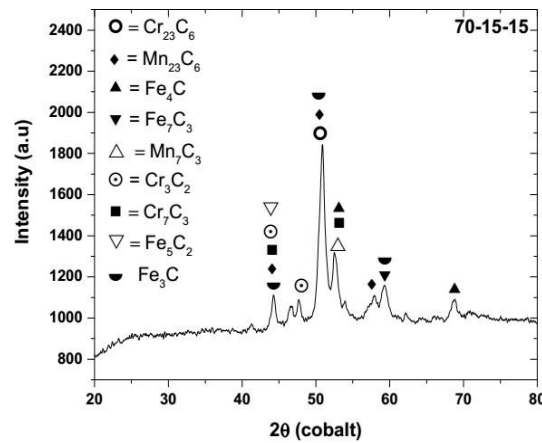
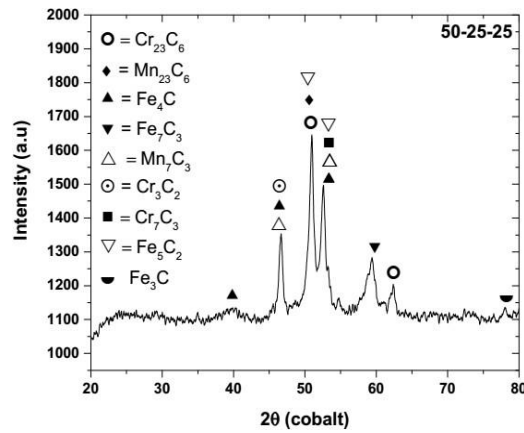
*Fig. 2. SEM images of a) sample 1 and b) sample 2.*

Preliminary XRD results are shown in Fig. 3a and Fig. 3b. Sample 1 has two forms of iron carbides, namely, cementite ( $\text{Fe}_3\text{C}$ ) and Hägg carbide ( $\text{Fe}_5\text{C}_2$ ).  $\text{Fe}_5\text{C}_2$  was prevalent in sample 1; cementite was dominant in sample 2. The software X'Pert Highscore plus was limited in its ability to reveal other carbides of iron and carbide formers, while crystallographic search-match software identified other carbide phases shown in Fig. 4a and Fig. 4b.



b)

Fig. 3. Diffractogram of a) sample 1 and b) sample 2



a)

b)

Fig. 4. Diffractogram using crystallographic search-match software:  
a) the sample 1, and b) sample 2

It can be deduced from the filtered diffractograms presented in Fig. 4a and Fig. 4b that similar carbides of Fe, Mn, and Cr were present in both samples 1 and 2. However,  $\text{Fe}_5\text{C}_2$  has the highest intensity in sample 1, while  $\text{Fe}_3\text{C}$  has the highest intensity in sample 2.

#### The hardness of hardfacing samples and discussions

Average Rockwell-C hardness values of samples 1 and 2 were 53.5 HRC and 54.9 HRC, while their corresponding Vickers hardness based on ASTM E140-97 hardness conversion were 567 HV and 592 HV, respectively. The high hardness value of sample 2 compared to sample 1 arose due to the higher chromium and carbon content of sample 2; which resulted in several carbides of chromium such as  $\text{Cr}_{23}\text{C}_6$ ,  $\text{Cr}_3\text{C}_2$ , and  $\text{Cr}_7\text{C}_3$ .

The hardness values recorded are in agreement with the observation of *Anand et al.* [25], that increase in chromium content, increases the hardness due to the formation of chromium carbide at the grain boundary. According to *Venkatesh et al.* [26], iron-based alloys with high chromium content result in high hardness and excellent abrasion resistance due to the increased presence of chromium carbide. *Buytoz and Yildirim* [27] noted that lower hardness values with small amounts of carbon and chromium in the microstructure, but high carbon and chromium content in carbide form results in excellent wear behavior.

#### Wear volumes of hardfacing samples and discussions

Densities of samples 1 and 2 are 7.25 g/cm<sup>3</sup>, and 7.06 g/cm<sup>3</sup>, and the wear volumes are 0.131 cm<sup>3</sup>, and 0.085 cm<sup>3</sup>, respectively. The wear volume of sample 1 is higher than that of sample 2, which is linked to their hardness values. Though the difference in their hardness is not significant, the hardness of sample 2 was higher than that of sample 1. This difference is associated with the high chromium and carbon content in sample 2 composition compared to sample 1.

The wear results for samples 1 and 2 are supported by *Pawar and Utpat* [28], who noted that addition of chromium in A487 stainless steel alloy improves hardness. *Kenchi Reddy and Thanusa* [29] found that wear resistance increases with increase in the percentage of chromium and carbon content in weld deposits. *Brezinová et al.* [30] noted that an electrode E518B with carbon content 3.4% and chromium 29% gave a hardness value of 660 HV, while E508 with 0.5% C, 6.0%Cr yielded a hardness value of 580 HV.

#### *Impact energies of the hardfaced samples and discussions*

The impact energies of the hardfaced samples prepared with samples 1 and 2 and the low carbon steel substrate were 30.0 J and 29.5 J, respectively. The average energy absorbed by hardfaced sample 1 is higher than that of hardfaced sample 2 due to the high manganese content of sample 1. This result is in agreement with the finding of *Zhang and Farrar* [31], who noted that increase in the manganese content of a weld metal increases toughness. The impact energy value of specimen 1 was expected to be higher than that of specimen 2, but the presence of chromium caused a reduction in the impact property. More so, *Surian et al.* [32] suggested that electrodes with high chromium content introduce increased hardness and reduced toughness of a weld.

#### *Selection of hardfacing composition*

Wear components used in abrasion, and low impact applications include crusher jaws, rolls, mantles and concave; these are usually made of high manganese austenitic steel. The hardness value of the non-deformed heat-treated Hadfield steel falls within 215 – 230 HV [33], which is lower than the hardness of samples 1 and 2. However, the selection of the hardfacing composition was based on the hardness, wear resistance, impact energy and cost of the alloying materials, as shown in Table 2.

*Table 2 Selection of hardfacing composition based on wear properties and cost*

Selection criteria	Sample 1	Sample 2	Preferred sample
Hardness (HV)	567	592	2
Wear volume (cm <sup>3</sup> )	0.131	0.085	2
Impact energy (J)	30.0	29.5	1
Alloy content (wt.%) – cost	47.5	30.9	2

Being the preferred sample for hardness, wear volume and alloy content criteria, sample 2 with Fe: Mn: Cr charge mass ratio 7: 1.5: 1.5 (70:15:15) becomes the chosen composition for actual production of the hardfacing alloy for high abrasion and low impact wear applications.

### **Conclusions**

- (i) The impact energy values of studied samples produced with charge mass ratios for Fe: Mn: Cr of 2: 1: 1 and 7: 1.5: 1.5 were very close, but the wear resistance of sample 2 is better due to its higher hardness. Additionally, both samples contain same carbides of iron, chromium, and manganese. While Hägg carbide was prevalent in the microstructure of the hardfacing produced by sand casting, cementite dominated the microstructure of the sample produced with open permanent molds.
- (ii) The consumable with lower alloy content is cheaper and preferable because of the cost of the alloying materials, and in this research, the sample was noticed to possess lower wear volume and higher hardness.
- (iii) The hardfacing alloy with mass charge ratio of 7: 1.5: 1.5 for Fe: Mn: Cr is recommended for use in high abrasion and low impact applications such as crusher jaws, cone crusher mantles and concaves and crusher rolls.

### **References**

- [1] B. Khanpara, P. Rathod: International Journal of Engineering Technology, Management and Applied Sciences, 5 (2017) 132-139.
- [2] K.M. Kenchi Reddy, C.T. Jayadeva, A. Sreenivasan: International Journal of Engineering Science and Innovative Technology, 3 (2014) 464-475.

**Frontiers in Mechanical, Mining and Material Engineering**  
**Volume 1 Issue 2 2025**

- [3] F. Haakonsen: Department of Material Science and Engineering, Norwegian University of Science and Technology, Trondheim, PhD Theses, 2009.
- [4] F. Scandella, J.-M. Bonnel: Soudage Et Techniques Connexes, 71 (2017) 37-48.
- [5] B. Nedeljković, V. Lazić, S. Aleksandrović, B. Kristić, M. Mutavdžić, D. Milosavljević, M. Đorđević: MJoM, 16 (2010) 77-90.
- [6] K.F. Dolman: Hardfacing Ferroalloy Materials, (2015) US Patent No. 8,941,032B2.
- [7] B. Maroli, S. Dizdar, S. Bengtsson, Iron based hardfacing alloys for abrasive and impactwear, [https://www.hoganas.com/globalassets/hoganas/business-areas/surface-coating/pm17-12-iron-based-hardfacing-alloys\\_maroli.pdf](https://www.hoganas.com/globalassets/hoganas/business-areas/surface-coating/pm17-12-iron-based-hardfacing-alloys_maroli.pdf), Accessed 28 October, 2017. R. Goel, G. Grewal: Indian Journal of Engineering & Materials Sciences, 31 (1996) 127-130.
- [8] V. Shibe, V. Chawla: Mechanica Confab, 2 (2013) 111-122.
- [9] B. Digambar, D. Choudhary: International Journal of Science and Research, 3 (2014) 2400-2402.
- [10] J. Kumar, H. Singh: International Journal of Engineering Research & Technology, 04 (2015) 1190-1194.
- [11] J. Huebner, P. Rutkowski, D. Kata, J. Kusiński: Arch Metall Mater, 62 (2017) 531- 538.
- [12] V. Shibe, V. Chawla: International Journal of Engineering and Technology, 9 (2017) 105-111.
- [13] P. Singh, T. Singh, D. Singh, A. Singh: International Journal of Engineering Development and Research, 5 (2017) 744-756.
- [14] K. Krauze, Ł. Bołoz, T. Wydro, K. Mucha: Mining – Informatics, Automation and Electrical Engineering, 529 (2017) 26-34.
- [15] S.-W. Choi, C. Lee, T. Ha, T.-H. Kang, S.-H. Chang, In: Proceeding Underground Mining Technology, Canada, Eds: Hudyma, M., Potvin, Y., Australian Centre for Geomechanics, Perth 2017, 637-644.
- [16] G.M. Evans: Welding Research Supplement, (1980) 67-75.
- [17] H. Vasudev: International Journal of Advance Research, Ideas and Innovation in Technology, 1 (2014) 101-105.
- [18] S. Chand, D. Madhusudhan, K. Premalatha, A. Fathima, S. Shakila: International Journal of Materials Science, 11 (2016) 17-25.
- [19] C.K. Ande: Department of Materials Science and Engineering, Delft University of Technology, Delft, The Netherlands. Published Doctoral Thesis, 2013.
- [20] M. Trepczyńska-Lent: Archives of Foundry Engineering, 16 (2016) 169-174.
- [21] T.A. Balliett, G. Krauss: Metallurgical Transactions A., 7A (1976) 81-86.
- [22] Y. Prawoto: Solid Mechanics for Materials Engineers: Principles and Applications of Mesomechanics, Lulu Enterprises Inc., Morrisville, U.S.A., 2014, 13-14.
- [23] M.M. Serna, E.R.B. Jesus, E. Galegg, L.G. Martinez, H.P.S. Corrêa, J.L. Rossi. Materials Science Forum, 530 – 531 (2006) 48-52.
- [24] T. Anand, A. Bansal, A. Malham: International Journal of Innovative Research in Science and Engineering, 2 (2016) 395- 400.
- [25] B. Venkatesh, K. Striker, V.S.V. Prabhakar: Procedia Materials Science, 10 (2015) 527-532.
- [26] S. Buytoz, M.M. Yildirim: Archives of Foundry Engineering, 10 (2010) 279- 286.
- [27] P. B. Pawar, A.A. Utpat, In: Proceedings ICRISEM'16. Eds: Mattsson, M.M.K., Sharma, A.K., Andhra Pradesh, A. R. Research Publication 2016, 119-125.
- [28] K.M. Kenchi Reddy, K. Thanusa: IOSR Journal of Mechanical and Civil Engineering, 13 (2016) 72 – 79.
- [29] J. Brezinová, D. Draganovská, A. Guzanová, P. Balog, J. Viňáš: Metals, 6 (2016) 1-12.
- [30] Z. Zhang, R.A. Farrar: Welding Research Supplement, (1997) 183 – 196.
- [31] E. Surian, J. Trotti, A. Cassanelli, L.A. De Vedia: Welding Research Supplement, (1994) 45-53.
- [32] L. Qian, X. Feng, F. Zhang: Materials Transactions, 52 (2011) 1623- 1628.



Creative Commons License

This work is licensed under a Creative Commons Attribution 4.0 International License.